Gene Expression Profiling of Differentiated Thyroid Neoplasms: Diagnostic and Clinical Implications

Sylvie Chevillard,[1] Nicolas Ugolin,[1] Philippe Vielh,[2] Katherine Ory,[1] Céline Levalois,[1] Danielle Elliott,[4] Gary L. Clayman,[3] and Adel K. El-Naggar[4]

[1]Laboratoire de Cancérologie Expérimentale, Commissariat á L'Energie Atomique, Direction des Sciences du Vivant, Département du Radiobiologie et Radiopathologie, Fontenay-aux-Roses Cedex France; [2]Département de Pathologie, Institut Gustave Roussy, Villejuif Cedex, France; Departments of [3]Head and Neck Surgery and [4]Pathology, The University of Texas M.D. Anderson Cancer Center, Houston, Texas

ABSTRACT

Purpose: **The purpose of this research was to identify novel genes that can be targeted as diagnostic and clinical markers of differentiated thyroid tumors.**

Experimental Design: **Gene expression analysis using microarray platform was performed on 6 pathologically normal thyroid samples and 12 primary follicular and papillary thyroid neoplasms. Microarrays containing probes for 5,760 human full-length cDNAs were used for hybridization with total RNA from normal and tumor thyroid samples labeled with Cy3-dUTP and Cy5-dUTP, respectively. Scanned array images were recorded, and data analysis was performed. Selected sets of differentially expressed genes were analyzed using quantitative real-time reverse transcription-PCR for verification.**

Results: **We identified 155 genes that differentiate histologically normal thyroid tissues from benign and malignant thyroid neoplasms. Of these 75 genes were differentiated between follicular neoplasms (adenoma and carcinoma) and the follicular variant of papillary carcinoma. Purely follicular neoplasms (adenomas and carcinomas) shared many genetic profiles, and only 43 genes were distinctly different between these tumors. Hierarchical cluster analysis also differentiated conventional papillary carcinoma from its follicular variant and follicular tumors. The differentially expressed genes were composed of members of cell differentiation, adhesion, immune response, and proliferation associated pathways. Quantitative real-time reverse transcription-PCR analysis of selected genes corroborated the microarray expression results.**

Conclusions: **Our study show the following: (1) differences in gene expression between tumor and nontumor bearing normal thyroid tissue can be identified, (2) a set of genes differentiate follicular neoplasm from follicular variant of papillary carcinoma, (3) follicular adenoma and carcinoma share many of the differentiated genes, and (4) gene expression differences identify conventional papillary carcinoma from the follicular variant.**

INTRODUCTION

Differentiated thyroid epithelial tumors represent a spectrum of morphologically and biologically diverse lesions. The follicular-derived neoplasms (adenoma, carcinoma, and the follicular variant of papillary carcinoma) manifest overlapping cytomorphologic features and not infrequently pose diagnostic and treatment difficulties (1–4). Previous molecular studies of thyroid tumors have been limited to individual or multiple targeted markers and have failed to define any diagnostic or prognostic markers (5–14). Novel approaches are needed to identify reliable markers for pathological classification and to predict disease progression.

Parallel analysis of gene expression by microarray techniques offers a large-scale platform for screening tumors for novel markers for potential clinical applications. Using this approach, the biological and the molecular characteristics of several neoplastic entities, including a few thyroid neoplasms, have been defined (15–17). To characterize the genetic events underlying the morphologic and biological heterogeneity of differentiated thyroid neoplasms, we performed gene expression analysis of histologically normal thyroid tissues from tumor- and nontumor-bearing resections and benign and malignant follicular and papillary neoplasms.

MATERIALS AND METHODS

Tumor Samples. The samples for this study were taken from primary thyroid neoplasms and 6 nontumorous thyroid tissues (4 with matched tumor specimens) accessioned in the Department of Pathology at The University of Texas M.D. Anderson Cancer Center from 1996 to 2000. The study protocol was approved by the Institutional Review Board committee. The tumors included 4 follicular adenoma, 3 follicular carcinoma, 3 follicular variants of papillary carcinomas, and 2 conventional papillary carcinomas. The tissues were harvested immediately on arrival at the pathology suite, placed in liquid nitrogen, and stored at −80°C until used. Histopathologic diagnosis was performed according to the WHO guidelines.

cDNA Collection and Probes. Our platform consisted of 5,760 full-length cDNA clones from the Soares human infant

Received 1/15/04; revised 5/11/04; accepted 6/22/04.
Grant support: PIC Curie-CEA, Electricité de France, European Commission contract FIS5–2002-00004 (GENRAD-T), The Kenneth Muller Professorship (A. K. El-Naggar), and the Specialized Programs of Research Excellence in Head and Neck Cancer (SPORE).
The costs of publication of this article were defrayed in part by the payment of page charges. This article must therefore be hereby marked *advertisement* in accordance with 18 U.S.C. Section 1734 solely to indicate this fact.
Requests for reprints: Adel K. El-Naggar, The University of Texas M.D. Anderson Cancer Center, Department of Pathology, 1515 Holcombe Boulevard, Houston, TX 77030. Phone: 713-792-3109; Fax: 713-792-5532; E-mail: anaggar@mdanderson.org.

brain 1NIB library (18) kindly provided by Genethon (Evry, France). Plasmids containing clones were grown in *Escherichia coli* by standard microbiologic methods. Each insert was (PCR) amplified (30 cycles) with vector primers derived by sampling 1 μL of cell culture. PCR products were purified by EtOH precipitation, washed in 70% EtOH, dried, dissolved in 1 mmol/L EDTA/10 mmol/L Tris-HCl (pH 8; TE)/DMSO at 50:50 concentration and stored at −80°C. The quality, size, and concentration of PCR products were determined after agarose gel electrophoresis using Genetools software (Syngene; Merck Eurolab, Fontenay-sous-Bois, France) and were automatically annotated in the final differential expression data file.

Arraying. PCR products were arrayed on poly-L-lysine-coated slides (Menzel Glaser: CML, Nemours, France) using the Microgrid II pro arrayer (Biorobotics Ltd., Cambridgeshire, United Kingdom). Slides were packed and stored in a dark, dry place at room temperature until use.

Array Hybridizations. Before hybridization, the slides were hydrated over boiled water, dried for 3 seconds at 80°C, and exposed to UV irradiation (300 mJ, 254 nm) for DNA cross-linking. Slides were immersed in a freshly prepared blocking solution consisting of succinic anhydride (0.02 mmol/L) dissolved in 150 mL of 1-methyl-2-pyrrolidinone and 17 mL of sodium borate (0.2 mol/L; pH 8) and placed in an orbital shaker for 20 minutes. Slides were washed in H_2O and were immersed in 100% EtOH at −20°C before a final 5-minute centrifugation at 500 rpm at room temperature. Slides were then prehybridized at 42°C in a 3× SSC, 0.1% SDS, 0.1% bovine albumin for 30 minutes at 42°C, washed in H_2O, and immersed and in isopropanol and absolute EtOH, successively. The slides were then centrifuged at 500 rpm for 5 minutes at room temperature.

RNA, cDNA, and Labeling. Total RNA was prepared using RNAplus according to the manufacturer's protocol (Q-Biogene, Illkirsch, France). For each competitive hybridization, total RNA from a clinical sample and the normal thyroid reference from Clontech (Palo Alto, CA) were labeled with Cy3-dUTP and Cy5-dUTP (Amersham Pharmacia Biotech, Saclay, France) by reverse transcription. For each reverse transcription reaction, 20 μg of RNA was mixed with random hexamer (pdN6, Amersham Pharmacia Biotech; 2.5 μg/mL) in a total volume of 15.5 μL, heated at 65°C for 10 minutes, and placed on ice for at least 5 minutes. Unlabeled nucleotide pool (final concentration 500 μmol/L each dATP, dCTP, dGTP, and 200 μmol/L dTTP), either Cy3 or Cy5 conjugated dUTP (final concentration 66 μmol/L; NEN, Saclay, France), 1× first-strand Superscript II buffer, 10 mmol/L DTT, and reverse transcription (400 U; Superscript II; Life Technologies, Inc., Cergy-Pontoise, France) were added to a final volume of 30 μL. After incubation at 42°C for 2 hours in a dark room, RNA was hydrolyzed by adding EDTA (45 mmol/L) and NaOH (180 mmol/L) and incubated at 65°C for 5 minutes. The mixture was neutralized by Tris-HCl (450 mmol/L; pH 7.5) and by adjusting the volume to 500 μL with Tris-EDTA. Labeled cDNA was purified by centrifugation in a Microcon YM-30 (Amicon; Millipore, Bedford, MA) and eluted twice with 40 μL of TE.

Hybridization. The Cy3 and Cy5-labeled cDNAs were mixed with 20 μg human Cot-1 DNA, 20 μg yeast tRNA (Life Technologies, Inc.) and 10 μg poly(A; Sigma-Aldrich, Saint-Quentin Fallavier, France), then precipitated with 0.5 volumes of 7.5 mol/L sodium acetate (pH 5.2) in EtOH. The pellet was dissolved in 60 μL of hybridization solution (50% formamide, 2.5× Denhardt's solution, 0.5% SDS, and 6× SSPE. The probe was heated for 2 minutes at 100°C, incubated at 37°C for 20 to 30 minutes, and placed between slide and coverslip. The arrays were incubated overnight at 42°C in a custom humidified slide chamber. The slides were then washed in a first bath of 0.1× SSC with 0.1% SDS for 5 minutes and then twice in 0.1× SSC for 5 minutes at room temperature. The arrays were dried by centrifugation at 600 rpm for 10 minutes. As recommended, each hybridization was performed twice with reverse labeling (dye-swap; refs. 19–21).

Image Analysis and Array Quantification. Arrays were scanned using a two-color laser confocal scanner (GMS 418, Genetic Microsystems, Woburn, MA). Independent images were acquired for Cy3 (532 nm) and Cy5 (635 nm). Each spot was defined by automatic positioning of a grid using image-analysis spot-tracking software (patent US 10/173,672 June, 19, 2002; CA 2,389,901 June, 20, 2002). Each signal intensity was integrated >15 to 20 μm square pixels and recorded in 16-bit format. For each spot and fluorochrome, the background and the signal pixels were segmented with a specific Expectation-Maximization algorithm, and finally the net signal intensity of a spot was obtained by subtracting calculated local background intensity from the signal intensity. The dye-swap hybridization allows us to estimate the reproducibility between the two independent measures obtained for either the reference thyroid or the clinical sample (21). A reliability factor was calculated to compare the two measurements of a given spot and to score the reproducibility of signal intensities obtained for ^{Cy3}C and ^{Cy5}C. The reliability factor (*i*) factor of the i^{th} spot is equal to the ratio of the two relative intensities measured for the i^{th} spot (or inverse ratio if >1).

For additional intermicroarray comparisons and for calculating the expression ratio "clinical sample/thyroid reference," the series of paired ^{Cy3}C and ^{Cy5}C measures (each being already scored with its reliability factor) were corrected on the line of slope 1, and normalization was performed according to a set of constantly expressed genes (22). A cutoff of 0.6 for reliability factor was used, considering that the two measures are reproducible.

The discrimination between two categories of samples, for example, thyroid adenomas and normal thyroid samples, is performed in two steps. The first step involves finding a set of genes that are differentially expressed within each category. The second step involves clusterizing samples according to this set of genes. The expression data are organized in a matrix N.P, where the N lines represent the genes and the P columns denote the samples. Each line of the matrix (vector line) is centered according to the following formula:

$$X'_{i,j} = X_{i,j} - \frac{1}{p}\sum_{j=1}^{p} X_{i,j}$$

and normalized according to:

$$X''_{i,j} = \frac{X'_{i,j}}{\sqrt{\sum_{j=1}^{p} X'^{2}_{i,j}}}$$

where *i* and *j* represent respectively the indexes of lines and columns of the N.P matrix. And *x* the expression value at the (*i,j*) position of the matrix. The centering allowed forthe analysis of a given gene, as a function of the mean of expressionof this gene, in all samples of the analyzed categories. This permits the determinations of each gene expression, sample per sample, in relation to the average of expression. The normalization step minimizes the differences in the fold expression level between samples and genes. Finally, we are able to compare each vector line according to the relative value of the difference in the level of expression without dealing with the level of expression itself.

Gene Clustering. To identify these genes that differentiate between two categories, we constructed two templates that represent the two theoretical vector lines. The first vector line has a value of 1 in all of the samples belonging to the first category and a value of −1 in samples belonging to the second category. The second vector line is the inverse of the first one with values of −1 in samples belonging to the first category and 1 for those belonging to the second category.

After centering and normalization of the data, the two templates and the experimental vector lines were clustered using locally developed software (ClusterIt, Paris, France)

All of the initiator vectors located at a weighted Euclidian distance inferior to a threshold *s* were grouped in the same cluster. If a vector also belonged to another cluster, there are two possible solutions. First, if this common vector is the initiator vector of one of the two clusters of interest then for each cluster, the mean of the vectors exclusively belonging to it is calculated. If the weighted Euclidian distance between the two means is inferior to the threshold S, the two clusters are grouped. If the distance is not inferior to the threshold, the two clusters are maintained as different clusters, and the common vectors are included in the nearest cluster (except if it is the initiator cluster). Secondly, if the common vector corresponds to a non-initiator vector, the vector is directly included in the closest cluster.

The threshold *s* is steadily decreased (s/100), and with each reduction, the same procedure is applied on each new cluster derived from the previous reduction. The initial threshold *s* is chosen such that

$$s = \frac{2}{\sqrt{p}}$$

corresponds to the highest distance existing between two centered and normalized vectors, where *p* is the number of columns of the matrix. The weighted Euclidian distance is defined as followed:

$$d(X''_{i,.}, X''_{i',.}) = \frac{1}{\sum_{j=1}^{p} W_{i,j}W_{i',j'}} \sum_{j=1}^{p} W_{i,j}W_{i',j'}(X''_{i,j}, X''_{i',j'})^2$$

where

$$X''_{i,.}$$

represents a vector line of the matrix,

$$X''_{i,j}$$

the expression of the gene *i* in condition *j* (centered and normalized value), and

$$W_{i,j}$$

a weighting factor between 0 and 1 proportional to the reproducibility of each expression value (dye-swap experiments). The values of template vector lines are arbitrarily fixed at a very high level to force the experimental vector lines to clusterize with the templates.

The final step of the cluster analysis corresponds to $s = 0$, then each cluster is composed of a unique vector line. By following step by step the evolution of the cluster composition, it is possible to determine the lineage of each cluster and to define a hierarchical tree as a function of the cluster composition. In that context, attention was given to the two clusters, including the two template vector lines. To define at which *s* value (*i.e.*, at what step), the composition of the cluster is homogeneous (see below), we developed two parameters *Cd* and *RSC* that permit the evaluation of cluster stability of a given:

$$Cd = \frac{\sigma_{\rho real \rho theoretical}}{\sigma_{\rho real}^{2}} \text{ and } RSC = \frac{\sqrt{n.\sum_{i=1}^{n} \overline{W_{i.}}(\rho_{real} - \rho_{theoretical})^2}}{\sum_{i=1}^{n_{class}} \overline{W_i}}$$

where:

$$\rho$$

represents the real or the theoretical densities of probability of the distribution of the *n* vectors within the considered class,

$$\sigma_{\rho real}$$

the SE of the real distribution of the vector in the considered class,

$$\sigma_{\rho real \rho theoretical}$$

the covariance computed between the real and the theoretical distributions of the vectors within the considered class, and

$$\overline{W_i} = \frac{\sum_{j=1}^{p} W_{i,j}}{p}$$

represents the average of the weighted values of a vector line of the *N.P* matrix.

The definition of *Cd* and *RSC* factors are based on the following hypothesis: using DNA microarray, the error in the measure follows a normal distribution. Thus, as soon as a class of genes is homogeneous, a normal distribution of the vectors around the mean of all vectors within the class is expected. At the first step the clustering, defined with a threshold

$$s = \frac{2}{\sqrt{p}},$$

, all of the gene vectors are grouped within the same cluster, and the mean vector of the entire cluster was null. The measured *Cd* could be >0.8 if the number of different vectors within the cluster is large enough to ensure, by hazard, a normal distribu-

tion. The observed distribution resulted in a mixture of different classes of genes. Along with the steps of clustering and as *s* decreased, affiliated clusters segment and the number of vectors per cluster decreased, thus minimizing the probability of normal distribution due to hazard. At this point, the *Cd* coefficient becomes small (<0.8), and the vectors do not follow a normal distribution, because the number of mixed classes is not large enough to ensure a normal distribution due to the hazard. As soon as *s* is small enough to ensure that vectors belong to the same cluster and are homogeneous, *Cd* increases >0.8, the cluster is considered stable, and the vectors follow a normal distribution. At this step, the clustering could be improved by searching for the minimal *RSC* and checking vector by vector for the loss or gain of cluster stability.

Specimen Clustering. Gene clusters, from the template vector line and the experimental vector lines, represent the set of genes that discriminate between two categories. For tumor classification, a new matrix excluding the previous template vector lines and adding two sample vector columns representing each of the two experimental categories were developed. The lines for the new columns were coded 1 for the first cluster of genes and -1 for the second cluster of genes. These two additional columns represent an experimental sample template for each category, whereas other columns correspond to the gene expression of the selected genes in each experimental sample. The vector lines of the transposed matrix organized around the vector template allowed for the construction of the hierarchical sample tree. For calculating the mean value of gene expression within each category, a matrix $N'.Q$ is defined for a given category, where the N' lines represent the genes and the Q columns the different samples within the chosen category. For each gene, the weighted mean of expression was calculated according to the following equation:

$$\overline{X_{i,.}} = X''_{i,j} - \frac{1}{\sum_{j=1}^{Q} W_{i,j}} \sum_{j=1}^{Q} W_{i,j} \cdot X''_{i,j},$$

where *i* and *j* represent, respectively, the indexes of lines and columns of the $N'.Q$ matrix. And *x* the expression value at the (*i*,*j*) position of the matrix.

The mean reproducibility factor is calculated according to the following equation:

$$\overline{W_{i,.}} = \frac{\sum_{j=1}^{Q} sign W_{i,j}}{Q}$$

with a sign "+" if

$$X_{i,j} > 0$$

>0 and "−" if

$$X_{i,j} < 0,$$

< 0, where *w* is a weighting value between 0 and 1 proportional to the reproducibility of the expression value *x*.

We also investigated whether the follicular variant of papillary carcinoma can be distinguished from conventional papillary carcinoma by constructing 2^p vectors (p being the number of tumors) with the coordinates randomly equal to 1 or -1. The se vectors were organized in amatrix *N.P*, where the *N* lines represent the genes and the *P* columns the tumors. The five papillary tumors were randomly organized in the matrix, where each gene represents a vector. Within the homogeneous clusters of genes, we looked for clusters presenting two distinct levels of gene expression within these groups of tumors. We identified all of the clusters that permit the discrimination of one tumor against four or two tumors against three. We then grouped clusters that identify the same tumor, and, finally, we retained the group of clusters occurring at the highest frequency. With a such procedure, we constructed a reduced matrix N'. *P* and transposed the matrix to classify the five papillary tumors.

Quantitative Real-Time Reverse Transcription-PCR. For several genes, mRNA expression was analyzed by real-time reverse transcription-PCR (ABI PRISM 7700 Sequence Detector apparatus, Applied Biosystems (Courtaboeuf, France). First-strand cDNA synthesis was described previously, reactions were performed using Syber green incorporation (SYBR Green PCR Core Reagent, Perkin-Elmer), and quantification was performed using the dedicated software (Gene Amp software, Perkin-Elmer). Quantification of each gene expression was calibrated using a reference standard curve obtained by serial dilutions of PCR product prepared from a mixture of cDNAs from normal and tumorous thyroid samples handled separately but concomitantly with clinical samples. Gene expression was normalized as a function of the expression of the 18S rRNA, as described previously (23, 24).

RESULTS

The patients and tumor characteristics are presented in Table 1. As criteria for inclusion in the analysis, each array spot must be well measured in all of the samples. Accordingly, 4,287 spots satisfied such requirement in all of the specimens and formed the basis for the analysis. Thresholds of 2 and 0.5 were used as the mean expression ratio, for over- or underexpressed genes compared with the normal thyroid tissue, respectively. In the first phase of the analysis, the centered mean ratio of expression (tumor/reference) in different samples for each of the normal, adenoma, and follicular and papillary carcinomas was calculated for each spot.

Comparing the 6 normal thyroid specimens to the standard thyroid reference, 186 and 92 genes were found to be under- and overexpressed, respectively. Fig. 1*A* represents the main biological classifications of the differentially expressed genes, which are composed of the cytoskeleton, cell adhesion, and cellular matrix-related genes. Signal transduction and immuno-response genes accounted for 12% and 15% of the differentially expressed genes, respectively.

To determine neoplastic-associated genes, differentially altered genes between histologically normal thyroid tissues of tumor- and nontumor-bearing cases were excluded from the analysis. Accordingly, 4,101 well-measured genes in all of the tumor specimens applying the same centered mean of expression ratio (tumor/reference) were used. The number of differentially expressed genes in adenomas and follicular and papillary carcinomas were 615, 222, and 172, respectively (Table 1). Fig. 1, *A–D* display the under- or overexpression of

Table 1 Patients and specimens characteristics of thyroid specimens analyzed

#	Age	Race	Sex	Size	Diagnostic	Lymph node status
1	52	W	M	2.0	Papillary Ca.	Negative
2	54	M	F	4.5	Follicular	Negative
3	59	B	F	0.7	Papillary Ca.	Positive (extensive)
4	32	A	F	1.5	Follicular	Negative
5 (178/F6)	34	W	M	4.5	Follicular	Positive (extensive)
6	25	M	F	2.5	Adenoma	Negative
7 (195/H8)	17	W	F	2.5	Adenoma	Negative
8 (318/E5)	43	W	F	2.5	Adenoma	Negative
9 (275/E3)	56	W	F	4.0	Adenoma	Negative
10	57	W	M	2.0	Follicular Ca.	Negative
11	47	W	M	5.5	Follicular Ca	Negative
12 (278/E5)	46	W	F	7.6	Follicular Ca.	Positive (extensive)
13N	52	M	F	5.5	Normal of # 1	
14 N	51	M	F	4.0	Normal	
15 N	44	M	F	2.0	Normal of # 2	
16 N	32	A	M	2.0	Normal of # 4	
17 N	51	W	M	Multiple	Normal of # 10	
18 N	70	M	F	Goiter	Normal	

Abbreviations: W: White; M: Mexican; B: Black; A: Asian; Ca., cancer.

known genes according to their putative biological functions in normal thyroid and different neoplastic categories. The differentially expressed genes in adenomas (B) overlapped with those between normal thyroid samples (A) and follicular carcinoma (C) but distinctly different from those in papillary carcinomas (D).

The gene differences between two tumors within a category were used to develop a strategy for the expression within a category independent of the expression ratio. In that strategy, a given gene can be used to discriminate between two categories without applying a strict cutoff if the expression ratio of this gene is as follows: (1) the same for all samples within a category, and (2) different between the two categories. As shown in Fig. 2, *A* and *B*, and Fig. 3, *A* and *B*, 23, 52, and 80 genes define adenoma from papillary carcinoma, follicular carcinoma from follicular variant of papillary carcinoma, and adenomas from follicular carcinomas, respectively. The differentially expressed genes classifying follicular adenomas from follicular carcinomas are listed in Table 2. Restricting gene clustering to the five papillary carcinomas, a set of genes (Table 3) differentiated the follicular variant from conventional papillary carcinomas (Fig. 3*B*).

Table 4 presents the quantitative real-time reverse transcription-PCR analysis of selected genes identified by microarray anal-

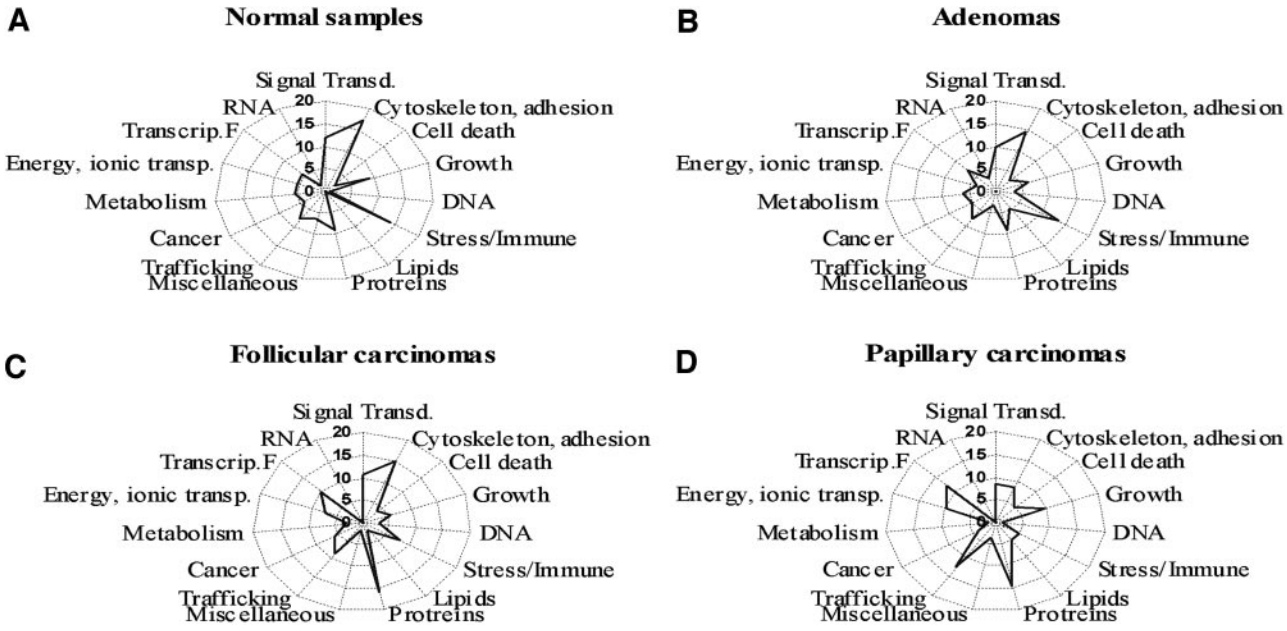

Fig. 1 Classification of differentially expressed genes according to their biological functions in normal thyroid samples (*A*), follicular adenomas (*B*), follicular carcinomas (*C*), and papillary carcinomas (*D*; expressed sequence tags or genes with unknown functions are not included).

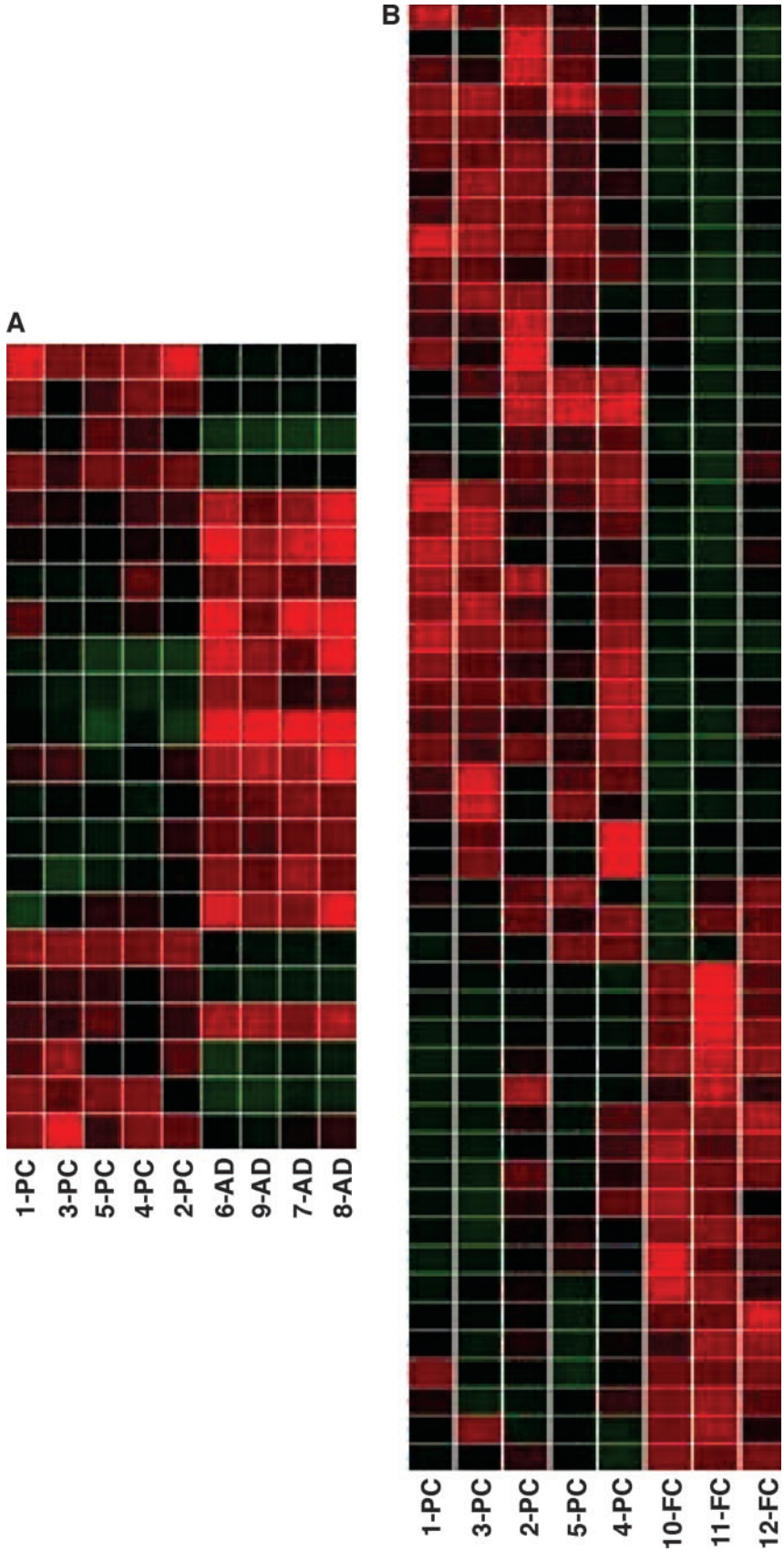

Fig. 2 Hierarchical clustering based on differentially expressed genes that distinguished adenomas (AD) from papillary carcinomas (PC) (*A*) and follicular carcinoma (FC) from papillary carcinomas (*B*), respectively.

Table 2 List of genes of which the expression permits to distinguish follicular adenomas from follicular carcinomas

Symbol	Name	Follicular expression ratio FC/FA	
		Under	Over
Cell cycle and proliferation			
	Cysteine-rich, angiogenic inducer, 61	0.05	
DUSP1	Dual specificity phosphatase 1	0.1	
VEGF	Vascular endothelial growth factor	0.3	
SNK	Serum-inducible	0.5	
GRN	Granulin		2
MCM7	Minichromosome maintenance deficient (*S. cerevisiae*) 7		3
Cell adhesion, shape and maintenance			
IMMT	Inner membrane protein, mitochondrial	0.2	
KRT8	Keratin 8	0.2	
EXT2	Exostose 2	0.5	
SEZ6L	Seizure related gene 6 (mouse)-like		2
CD47	CD47 antigen		3
NF2	Neurofibromin 2		3
Apoptosis			
BNIP3	BCL2 interacting protein 3	0.3	
Protein metabolism, catabolism and modification			
PPP1R14C	Protein phosphatase 1 regulatory (inhibitor) subunit 14C	0.2	
SRR	Serine racemase	0.3	
PRKACB	Protein kinase-cyclic AMP-dependent catalytic β	0.3	
DUSP5	Dual specificity phosphatase 5	0.3	
UBE2V1	Ubiquitin-conjugating enzyme E2 variant 1	0.4	
DNAJB1	DNAJ (Hsp40) homolog, subfamily B, member 1	0.4	
PKIA	Protein kinase (cyclic amp-dependent, catalytic) inhibitor α	0.4	
PACE4	Paired basic amino acid cleaving system 4	0.4	
EIF2AK3	Eukaryotic translation initiation factor 2 αkinase 3	0.5	
USP7	Ubiquitin specific protease 7		2
QPCT	Glutaminyl-peptide cyclotransferase		4
Signal transduction			
FLJ10521	Highly similar to rho guanyl nucleotide exchange factor	0.4	
RAP2A	RAP2A		4
ADCY1	Adenylate cyclase 1		4
CASR	Calcium-sensing receptor	0.5	
DNA metabolism maintenance and repair			
APEX	Multifunctional DNA repair enzyme	0.2	
Cytokine, inflammation, immune response			
SCGB1A1	Secretoglobin	0.1	
PSG7	Pregnancy specific β-1-glycoprotein 7		3
Transcription factor			
ID4	Inhibitor of DNA binding 4	0.2	
ZFX	Zinc finger protein, X-linked	0.30	
MEIS2	Meis (mouse) homolog 2		2
Ion/metal binding and transport			
SELENBP1	Selenium binding protein 1	0.3	
TFRC	Transferrin receptor	0.4	
SLC1A1	Solute carrier family 1 1	0.5	
AQP4	Aquaporin 4	0.5	
HPCAL4	Hippocalcin-like protein 4		3
Transport, trafficking secretory pathway			
ARL1	ADP-ribosylation factor-like 1	0.4	
GOLGB1	Golgi autoantigen	0.5	
Divers metabolism			
ACACA	Acetyl-Coenzyme A carboxylase α	0.5	
CKR	Glucokinase (hexokinase 4) regulatory protein	0.5	

ysis. The results confirm the cDNA expression level of these genes in different tumors.

DISCUSSION

Our study identified 186 (94 expressed sequence tags and 92 known genes) differentially expressed genes between normal tissues from tumor- and nontumor-bearing thyroid glands. Interestingly, the differentially expressed genes shared similar biological functions with those identified in follicular adenomas and included cytoskeleton, cell adhesion, cellular matrix, immune response stress-related, and signal transduction genes families. This finding, the first to our knowledge, suggests that

Table 3 List of genes whose expression permits to distinguish follicular variants of papillary carcinomas (FVPC) from papillary carcinomas (PC)

Symbol	Name	Expression ratios FVPC/PC	
		Under	Over
Cell cycle and proliferation			
CDK5R1	Cyclin-dependent kinase 5, regulatory subunit 1 (p35)	0.2	
FAT2	FAT tumor suppressor (Drosophila) homolog 2		2
CSE1L	CSE1 chromosome segregation 1-like (yeast)		2
CCND1	Cyclin D1		3
ZNF151	Zinc finger protein 151 (pHZ-67)		3
MAT2B	Methionine adenosyltransferase II, β		3
NUDEL	LIS1-interacting protein NUDEL; endooligopeptidase A		3
CDK2AP1	CDK2-associated protein 1		3
CENPC1	Centromere protein C 1		4
Cell adhesion, shape and maintenance			
APLP1	Amyloid beta (A4) precursor-like protein 1	0.5	
TYRO3	TYRO3 protein tyrosine kinase		2
WNT7B	Wingless-type MMTV integration site family, member 7B		2
ADD1	Adducin 1 (α)		2
SCARB1	Scavenger receptor class B, member 1		2
PSK-1	Type I transmembrane receptor (seizure-related protein)		3
LAD1	Ladinin 1		3
KRT19	Keratin 19		3
SPARC	Secreted protein, acidic, cysteine-rich (osteonectin)		3
CNN3	Calponin 3, acidic		3
GJA8	Gap junction protein, α8, 50kD		4
DSP	Desmoplakin		4
MSN	Moesin		4
MAP4	Microtubule-associated protein 4		4
SSPN	Sarcospan (Kras oncogene-associated gene)		4
MGEA5	Meningioma expressed antigen 5 (hyaluronidase)		5
SDC4	Syndecan 4 (amphiglycan, ryudocan)		9
Apoptosis			
PDCD2	Programmed cell death 2		2
PDCD6IP	Programmed cell death 6-interacting protein		3
Protein metabolism, catabolism and modification			
RPL35A	Ribosomal protein L35a	0.4	
COPS3	COP9 subunit 3	0.5	
DPP6	Dipeptidylpeptidase VI		2
PSMA5	Proteasome subunit, α type, 5		2
PSMD1	Proteasome 26S subunit, non-ATPase, 1		2
P5CR2	Pyrroline 5-carboxylate reductase isoform		2
PEPD	Peptidase D		2
FURIN	Furin (paired basic amino acid cleaving enzyme)		2
SIAH1	Seven in absentia homolog 1 (Drosophila)		2
UBAP2	Ubiquitin associated protein 2		2
PTK9	Protein tyrosine kinase 9		2
DDOST	Dolichyl-diphosphooligosaccharide-protein glycosyltransferase		2
THTPA	Thiamine triphosphatase		2
GCC1	Golgi coiled coil 1		2
EIF4A1	Eukaryotic translation initiation factor 4A, isoform 1		3
SGT	Small glutamine-rich tetratricopeptide repeat (TPR)-containing		3
DNAJA4	DnaJ (Hsp40) homolog, subfamily A, member 4		3
AANAT	Arylalkylamine N-acetyltransferase		4
EIF3S7	Eukaryotic translation initiation factor 3, subunit 7		4
DPP3	Dipeptidylpeptidase III		5
RPL19	Ribosomal protein L19		6
RPS25	Ribosomal protein S25		9
UBE3A	Ubiquitin protein ligase E3A		11
RPL7A	Ribosomal protein L7a		22
Signal transduction			
NTRK2	Neurotrophic tyrosine kinase, receptor, type 2	0.2	
FGFR1	Fibroblast growth factor receptor 1	0.5	
GRB2	Growth factor receptor-bound protein 2		2
FREQ	Frequenin (Drosophila) homolog		2
ITPK1	Inositol 1,3,4-triphosphate 5/6 kinase		2
DAB2IP	DAB2 interacting protein		2
NOTCH2	Notch homolog 2		2

Table 3 Continued

Symbol	Name	Expression ratios FVPC/PC Under	Over
CENTA1	Centaurin, α 1		2
KIAA0720	KIAA0720 protein		2
GNG12	Guanine nucleotide binding protein, gamma 12		2
PTPRE	Protein tyrosine phosphatase, receptor type, E		3
ARHGEF12	Rho guanine exchange factor (GEF) 12		3
GNAZ	Guanine nucleotide binding protein, α z polypeptide		3
PPAP2C	Phosphatidic acid phosphatase type 2C		3
AIP	Aryl hydrocarbon receptor-interacting protein		4
DGKA	Diacylglycerol kinase, α (80kD)		4
GNAL	Guanine nucleotide binding protein		4
ARHA	Ras homolog gene family, member A		4
EPHB1	Receptor for members of the ephrin-b family		5
GPR51	G protein-coupled receptor 51		5
YWHAE	Tyrosine 3-monooxygenase		5
NR0B2	Nuclear receptor subfamily 0, group B, member 2		7
NTRK3	Neurotrophic tyrosine kinase, receptor, type 3		7
DNA metabolism maintenance and repair			
ERCC2	Excision repair complementation group 2 (XPD)		2
DGUOK	Deoxyguanosine kinase		2
RPA1	Replication protein A1 (70kD)		3
RFC1	Replication factor C (activator 1) 1 (145kD)		3
POLG	Polymerase (DNA directed), γ		3
CGGBP1	CGG triplet repeat binding protein 1		4
NME2	Nonmetastatic cells 2, protein (NM23B) expressed in		13
Cytokine, inflammation, immune response			
FCER2	Fc fragment of IgE, low affinity II, receptor for (CD23A)	0.2	
CSF1	Colony stimulating factor 1	0.4	
BAP29	B-cell receptor-associated protein BAP29	0.5	
TNFRSF25	Tumor necrosis factor receptor superfamily, member 12a		3
TNF	Tumor necrosis factor (TNF superfamily, member 2)		4
LNK	Lymphocyte adaptor protein		5
HLA-DQA1	Major histocompatibility complex, class II, DQ α1		6
Transcription factor			
HOXC6	Homeo box C6	0.1	
ID4	Inhibitor of DNA binding 4	0.4	
TRIM28	Tripartite motif-containing 28		2
CUTL1	Cut-like 1, CCAAT displacement protein (Drosophila)		2
MSL3L1	Male-specific lethal 3-like 1 (Drosophila)		3
SNW1	SKI-interacting protein		3
E4F1	E4F transcription factor 1		3
CGBP	CpG binding protein		3
JUNB	Jun B proto-oncogene		4
ASCL1	Mammalian achaete-scute homolog-1		4
ISGF3G	Interferon-stimulated transcription factor 3, γ (48kD)		5
HCNGP	Transcriptional regulator protein		6
HCNP	tetratricopeptide repeat protein involved in transcription		6
SSX1	Synovial sarcoma, X breakpoint 1		19
Ion/metal binding and transport			
ZNT6	Likely ortholog of mouse zinc transporter 6	0.3	
KCNF1	Potassium voltage-gated channel, subfamily F, member 1	0.4	
SELENBP1	Selenium binding protein 1	0.5	
SLC12A4	Solute carrier family 12 potassium/chloride transporters		2
VSNL1	Visinin-like 1		3
NDUFS4	NADH dehydrogenase (ubiquinone) Fe-S protein 4 (18kD)		3
ANXA5	Annexin A5		3
ATP2B2	ATPase Ca++		3
CPNE7	Copine VII		5
Transport, trafficking secretory pathway			
KPNA4	Karyopherin α 4 (importin α 3)		2
RABEX5	Putative Rab5 GDP/GTP exchange factor homologue		2
SYT11	Synaptotagmin XI		2
ENTH	Enthoprotin		2
ABCC8	ATP-binding cassette, subfamily C (CFTR/MRP), member 8		2
ALS2CR3	ALS2CR3, KIAA0549, CALS-C		2
ABCF2	ATP-binding cassette, subfamily F (GCN20), member 2		2
SV2	Likely ortholog of mouse synaptic vesicle glycoprotein 2a		3
VAPA	Vesicle-associated membrane protein)-associated A		3

Table 3 Continued

Symbol	Name	Expression ratios FVPC/PC Under	Over
ARCN1	Archain 1		3
Diverse metabolism			
GLO1	Glyoxalase I	0.5	
UGP2	UDP-glucose pyrophosphorylase 2		2
PC	Pyruvate carboxylase		2
TALDO1	Transaldolase 1		4
CYP51	Cytochrome P450, family 51		6
Stress			
PXR1	Peroxisome receptor 1		2
OSR1	Oxidative-stress responsive 1		6
CIRBP	Cold inducible RNA binding protein		6
RNA			
SRRM1	Serine/arginine repetitive matrix 1	0.5	
QKI	Homolog of mouse quaking QKI		2
PPP1R8	Protein phosphatase 1, regulatory (inhibitor) subunit 8		2
Miscellaneous			
PEG10	PateRNAlly expressed 10		2
DGS-A	DiGeorge syndrome gene A		2
BGLAP	Bone γ-carboxyglutamate (gla) protein (osteocalcin)		2
SDNSF	Neural stem cell derived neuronal survival protein		2
PLP1	Proteolipid protein 1 (Pelizaeus-Merzbacher disease)		2
TAZ	Tafazzin (cardiomyopathy, dilated 3A (X-linked)		2

thyroid tissue, from thyroid tumor-bearing patients, manifests genomic instability due to either engagement in the field of tumorigenesis or in response to tumor proximity.

The data also show that adenomas can be differentiated from follicular carcinomas by a set of 43 genes of known functions. Of these, 10 were reported previously (17) to be highly expressed in follicular carcinomas (PEG10, PLCB4, FBN1, ID4, DUSP1, NID, BSG, CBS, HXB, RPP1, and TRAP240) and 3 genes (SORD, X123, MCG14797) in follicular adenomas (25, 26). Granulin, a putative growth factor, was noted to be significantly overexpressed in carcinomas compared with adenomas. Previous studies of glioblastoma and gastric and ovarian cancers have also shown an up-regulation of this gene (27–29). Of the down-regulated genes, *DUSP 1,* which has known proliferation and differentiation functions, has been shown previously to be down-regulated in follicular carcinomas (17) and in advanced epithelial ovarian cancer (30). We also noted the *PKIA* gene, a potent inhibitor of protein kinase B, to be down-regulated in follicular carcinomas compared with adenomas, supporting previous molecular studies of sporadic thyroid cancer (31). As in earlier studies, the *VEGF* gene was characteristically noted in follicular carcinomas (32, 33).

Our study identified a set of 23 and 52 genes that differ-

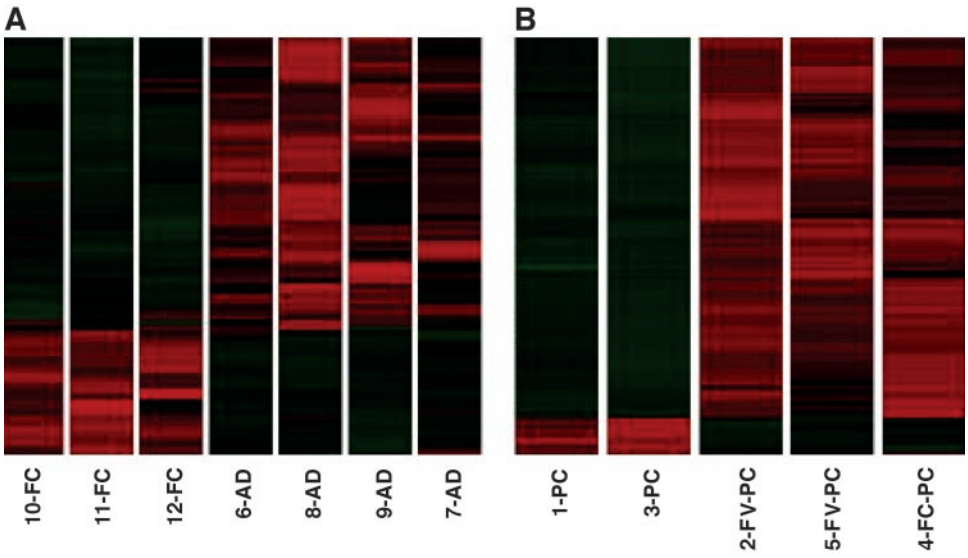

Fig. 3 Hierarchial clustering based on differentially expressed genes that segregate follicular carcinomas (FC) from adenomas (AD) and papillary carcinoma (PC) from follicular variant of papillary carcinomas (FV PC; *B*), respectively. Details of genes with known functions are given on Tables 3 and 4.

Table 4 Analysis of gene expression of DUSP5, CYR61, and SDC4 by real time RT-PCR

Gene	Follicular							Papillary				
	Adenomas				Carcinomas			TP	FV	TP	FV	FV
	6	7	8	9	10	11	12	1	2	3	4	5
DUSP5	2.2	2.3	2.2	2.3	1	1.3	1.4	5	5	1.8	13	4
CYR61	7.5	21	14	15	2	1	0.8	3	0.6	7	2	0.5
SDC4	1.6	3.2	1	1.6	0.8	4	5.8	5	31	13	37	20

NOTE. Results were normalized as compared to the quantity of 18S RNA.

Abbreviations: TP, true papillary carcinomas; FV, follicular variant of papillary carcinomas.

entiated papillary carcinoma from both follicular adenomas and carcinomas, respectively (Fig. 2, *A* and *B*). These genes were composed of members of the protein metabolism/catabolism (15%), intracellular trafficking (12%), ion/metal binding and transport proteins (10%), and transcription related (12%) gene families. The *Cyr61* gene was underexpressed in both papillary and follicular carcinomas (Fig. 2*A*) compared with adenomas, and it was shown previously to be down-regulated in papillary carcinomas (16). Also *MCM7*, a DNA replication gene, was overexpressed in papillary carcinomas compared with adenomas. Although, the overall gene expressions of papillary and follicular carcinoma (Fig. 1) showed common features, we identified individual genes that differentiate between papillary and follicular carcinomas. Among these are the DUSP6 and DUSP5, members of the dual-specificity phosphatase gene family. DUSP5 has been reported previously to be up-regulated in premalignant lesions and underexpressed in invasive pancreatic carcinoma (34). The *MFGE8* gene that plays a key role in activities such as cell motility, activation, contact, and the maintenance of the membrane is also highly expressed in papillary carcinomas compared with adenomas. *MFGE8* was shown previously to be highly overexpressed in human breast tumors (35).

Gene cluster analysis additionally segregated the conventional form from the follicular variant of papillary carcinomas (Fig. 3*B*). Fourteen of these genes had transcriptional functions and included 2 of the Id4 and HOXC6, down-regulated and 12 (*TRIM28, CUTL1, MSL3L1, SNW1, E64F1, CGBP, JUNB, ASCL1, IFGS3G, HCNGP, HCNP*, and *SSX1*) overexpressed. Only a few of these genes have been reported previously to be associated with thyroid gland development. The Id4 expression, a dominant-negative transcriptional regulator, is known to be mainly expressed in thyroid (26) and to induce cell proliferation and inhibit differentiation induced by thyroid hormone (36). The *NR0B2* gene, a negative regulator of receptor-dependent signaling pathways, interacts with thyroid hormone and retinoid and thyroid hormone receptors to repress nuclear hormone receptor-mediated transactivation (37).

Interestingly, the human *ACSL1/HASH1* gene, a transcription factor that is overexpressed in the follicular variant of papillary carcinoma, has also been reported to be highly expressed in neuroendocrine tumors, including medullary thyroid and small cell lung cancers (38). The finding suggests that the follicular variant, in contrast to the conventional form, preferentially manifest neuroendocrine features. The finding of under- and overexpression of the *NTRK2* and *NTRK3* genes, respectively (Table 4), and reports of medullary thyroid carcinoma support this hypothesis (39). Similarly, the *2NF151/MIZ2I, CDK2API*, and *P12DOC-I* genes, which are involved in cell proliferation (40, 41), were found to be overexpressed in follicular variants than in conventional papillary carcinomas. The *PEG10* gene was distinctly overexpressed in the follicular variant compared with the conventional papillary carcinoma. This gene has been reported to be highly expressed in hepatocellular carcinomas (42) and was found to differentiate follicular thyroid tumors from normal thyroid (17). Cyclin D1 (CCND1), a regulatory subunit of CDK4 or CDK6, has been found to be overexpressed in papillary thyroid carcinomas (43) and predicts lymph node metastases in papillary thyroid carcinoma (44).

In addition, the *BGLAP, SPARC*, and *MSN* genes, which bind to the Osteopontin (*OPN*) gene, were found to be distinctly overexpressed in the follicular variant of papillary carcinoma. These genes play a prominent role in bone and calcium metabolism and the formation of psammoma bodies in meningiomas (45) and ovarian serous papillary (46) and thyroid carcinomas (47). In addition, SPARC and MSN are also associated with tumor invasiveness and metastasis (48, 49). Tumor necrosis factor, a proinflammatory cytokine, TNFRSF25, a receptor expressed preferentially in tissues enriched with lymphocytes, NOTCH2, furin (PACE-1), GRB2, LNK, and HLA-DRB1 and HLA-DQA1, MHC-class II, were also overexpressed in follicular variants compared with papillary carcinomas. The expression of MHC class II was reported previously to be altered in papillary carcinomas, including the follicular variant (50).

Our study shows that gene expression array analysis correlated generally with classification of thyroid tumors. We also identified a set of genes that are differentially expressed between follicular benign and malignant neoplasms and between these tumors and papillary carcinoma. Although interesting, the final verification of the true biological nature must await additional follow-up on these patients.

REFERENCES

1. Fagin JA. Perspective lesions learned from molecular genetic studies of thyroid cancer—insights into pathogenesis and tumor-specific therapeutic targets. Endocrinology 2002;143:2025–8.

2. Links TP, van Tol KM, Meerman GJ, deVries EG. Differentiated thyroid carcinoma: a polygenic disease. Thryoid 2001;11:1135–40.

3. Brennan MD, Bergstralh EJ, van Heerden JA, McConahey WM. Follicular thyroid cancer treated at the Mayo Clinic 1946 through 1970: initial manifestations pathologic findings, therapy, and outcome. Mayo Clin Proc 1991;66:11–22.

4. Wanebo HJ, Andrews W, Kaiser DL. Thyroid cancer: some basic considerations. CA Cancer J Clin 1983;33:87–97.

5. Fukushima T, Suzuki S, Mashiko M, et al. BRAF mutations in papillary carcinomas of the thyroid. Oncogene 2003;22:6455–7.

6. Wiseman SM, Loree TR, Rigual NR, et al. Papillary thyroid cancer: high inter-(simple sequence repeat) genomic instability in a typical indolent cancer. Head Neck 2003;25:825–32.

7. Nikiforova MN, Biddinger PW, Caudill CM, Kroll TG, Nikiforov YE. PAX8-PPARgamma rearrangement in thyroid tumors: RT-PCR and immunohistochemical analyses. Am J Surg Pathol 2002;26:1016–23.

8. Garcia-Rostan G, Camp RK, Herrero A, Carcangiu M, Rimm DL, Tallini G. Beta-catenin dysregulation in thyroid neoplasms down-regulation, aberrant nuclear expression, a CTNNB1 exon 3 mutations are markers for aggressive tumor phenotypes and poor prognosis. Am J Pathol 2001;158:987–96.

9. Masood S, Auguste LJ, Westerband A, Belluco C, Valderama E, Attie J. Differential oncogenic expression in thyroid follicular and Hurthle cell carcinomas. Am J Surg 1993;166:366–8.

10. Hoos A, Stojadinovic A, Singh B, et al. Clinical significance of molecular expression profiles of Hurthle cell tumors of the thyroid gland analyzed via tissue microarrays. Am J Pathol 2002;160:175–83.

11. Frisk T, Kytola S, Wallin G, Zedenius J, Larsson C. Low frequency of numerical chromosomal aberrations in follicular thyroid tumors detected by comparative genomic hybridization. Genes Chromosomes Cancer 1999;25:349–53.

12. Takahashi M. Oncogenic activation of the ret protooncogene in thyroid cancer. Crit Rev Oncog 1995;6:35–46.

13. Yeh JJ, Marsh DJ, Zedenius J, et al. Fine-structure deletion mapping of 10q22–24 identifies regions of loss of heterozygosity and suggests that sporadic follicular thyroid adenoma and follicular thyroid carcinomas develop along distinct neoplastic pathways. Gene chromosomes Cancer 1999;26:322–8.

14. Rodrigues-Serpa A, Catarino A, Soares J. Loss of heterozygosity in follicular and papillary thyroid carcinomas. Cancer Genet Cytogenet 2003;141:26–31.

15. Huang Y, Prasad M, Lemon WJ, et al. Gene expression in papillary thyroid carcinoma reveals highly consistent profiles. Proc Natl Acad Sci USA 2001;98:15044–9.

16. Wasenius VM, Hemmer S, Kettunen E, Knuutila S, Franssila K, Joensuu H. Hepatocyte growth factor receptor, matrix metalloproteinase-11, tissue inhibitor of metalloproteinase-1, and fibronectin are upregulated in papillary thyroid carcinoma: a cDNA and tissue microarray study. Clin Cancer Res 2003;9:68–75.

17. Barden CB, Shister KW, Zhu B, et al. 3rd, Classification of follicular thyroid tumors by molecular signature: results of gene profiling. Clin Cancer Res 2003;9:1792–800.

18. Soares MB, Bonaldo MF, Jelene P, Su L, Lawton, L, Efstratiadis A. Construction and characterization of a normalized cDNA library. Proc Natl Acad Sci USA, 1994;91:9228–32.

19. Lee ML, Kuo FC, Whitmore GA, Sklar J. Importance of replication in microarray gene expression studies: statistical methods and evidence from repetitive cDNA hybridizations. Proc Natl Acad Sci USA 2000: 97;9834–9.

20. Schulze A, Downward J. Analysis of gene expression by microarrays: cell biologist's gold mine or minefield? J Cell Sci 2000;113;4151–6.

21. Tu Y, Stolovitzky G, Klein U. Quantitative noise analysis for gene expression microarray experiments. Proc Natl Acad Sci USA 2002;99: 14031–6.

22. Tseng GC, Oh MK, Rohlin L, Liao JC, Wong WH. Issues in cDNA microarray analysis: quality filtering, channel normalization, models of variations and assessment of gene effects. Nucleic Acids Res 2001;29: 2549–57.

23. Ory K, Lebeau J, Levalois C, et al. Apoptosis inhibition mediated by medroxyprogesterone acetate treatment of breast cancer cell lines. Breast Cancer Res Treat 2001;68:187–98.

24. Bishay K, Ory K, Olivier MF, Lebeau J, Levalois C, Chevillard S. DNA damage-related RNA expression to assess individual sensitivity to ionizing radiation. Carcinogenesis 2001;22:1179–83.

25. Ishibashi T, Bottaro DP, Michieli P, Kelley CA, Aaronson SA. A novel dual specificity phosphatase induced by serum stimulation and heat shock. J Biol Chem 1994;269:29897–902.

26. Rigolet M, Rich T, Gross-Morand MS, Molina-Gomes D, Viegas-Pequignot E, Junien C. cDNA cloning, tissue distribution and chromosomal localization of the human ID4 gene. DNA Res 1998;5:309–13.

27. Markert JM, Fuller CM, Gillespie GY, et al. Differential gene expression profiling in human brain tumors. Physiol Genomics 2001;5:21–33.

28. Line A, Stengrevics A, Slucka Z, Li G, Jankevics E, Rees RC. Serological identification and expression analysis of gastric cancer-associated genes. Br J Cancer 2002;86:1824–30.

29. Jones MB, Michener CM, Blanchette JO, et al. The granulin-epithelin precursor/PC-cell-derived growth factor is a growth factor for epithelial ovarian cancer. Clin Cancer Res 2003;9:44–51.

30. Manzano RG, Montuenga LM, Dayton M, et al. CL100 expression is down-regulated in advanced epithelial ovarian cancer and its re-expression decreases its malignant potential. Oncogene 2002;21:4435–47.

31. Sandrini F, Matyakhina L, Sarlis NJ, et al. Regulatory subunit type I-alpha of protein kinase A (PRKAR1A): a tumor-suppressor gene for sporadic thyroid cancer. Genes Chromosomes Cancer 2002;35:182–92.

32. Huang SM, Lee JC, Wu TJ, Chow NH. Clinical relevance of vascular endothelial growth factor for thyroid neoplasms. World J Surg 2001;25:302–6.

33. Lewy-Trenda I, Wierzchniewska-Lawska A. Expression of vascular endothelial growth factor (VEGF) in human thyroid tumors. Pol J Pathol 2002;53:129–32.

34. Furukawa T, Sunamura M, Motoi F, Matsuno S, Horii A. Potential tumor suppressive pathway involving DUSP6/MKP-3 in pancreatic cancer. Am J Pathol 2003;162:1807–15.

35. Carmon L, Bobilev-Priel I, Breener B, et al. Characterization of novel breast carcinoma-associated BA46-derived peptides in HLA-A2.1/D(b)-beta2m transgenic mice. J Clin Investig 2002;110:453–62.

36. Kondo T, Raff M. The Id4 HLH protein and the timing of oligodendrocyte differentiation. EMBO J 2000;19:1998–2007.

37. Seol W, Hanstein B, Brown M, Moore DD. Inhibition of estrogen receptor action by the orphan receptor SHP (short heterodimer partner). Mol Endocrinol 1998;12:1551–7.

38. Ball DW, Azzoli CG, Baylin SB, et al. Identification of a human achaete-scute homolog highly expressed in neuroendocrine tumors. Proc Natl Acad Sci USA 1993;90:5648–52.

39. Gimm O, Dziema H, Brown J, et al. Mutation analysis of NTRK2 and NTRK3, encoding 2 tyrosine kinase receptors, in sporadic human medullary thyroid carcinoma reveals novel sequence variants. Int J Cancer 2001;92:70–4.

40. Peukert K, Staller P, Schneider A, Carmichael G, Hanel F, Eilers M. An alternative pathway for gene regulation by Myc. EMBO J 1997;16: 5672–86.

41. Shintani S, Mihara M, Terakado N, et al. Reduction of p12DOC-1 expression is a negative prognostic indicator in patients with surgically resected oral squamous cell carcinoma. Clin Cancer Res 2001;7:2776–82.

42. Okabe H, Satoh S, Furukawa Y, et al. Involvement of PEG10 in human hepatocellular carcinogenesis through interaction with SIAH1. Cancer Res 2003;63:3043–8.

43. Kim JY, Cho H, Rhee BD, Kim HY. Expression of CD44 and cyclin D1 in fine needle aspiration cytology of papillary thyroid carcinoma. Acta Cytol 2002;46:679–83.

44. Khoo ML, Beasley NJ, Ezzat S, Freeman JL, Asa SL. Overexpression of cyclin D1 and underexpression of p27 predict lymph node metastases in papillary thyroid carcinoma. J Clin Endocrinol Metab 2002;87:1814–8.

45. Hirota S, Nakajima Y, Yoshimine T, et al. Expression of bone-related protein messenger RNA in human meningiomas: possible involvement of osteopontin in development of psammoma bodies. J Neuropathol Exp Neurol 1995;54:698–703.

46. Maki M, Hirota S, Kaneko Y, Morohoshi T. Expression of osteopontin messenger RNA by macrophages in ovarian serous papillary cystadenocarcinoma: a possible association with calcification of psammoma bodies. Pathol Int 2000;50:531–5.

47. Tunio GM, Hirota S, Nomura S, Kitamura Y. Possible relation of osteopontin to development of psammoma bodies in human papillary thyroid cancer. Arch Pathol Lab Med 1998;122:1087–90.

48. Carmeci C, Thompson DA, Kuang WW, Lightdale N, Furthmar H, Weigel RJ. Moesin expression is associated with the estrogen receptor-negative breast cancer phenotype. Surgery (St Louis) 1998;124:211–7.

49. Rempel SA, Ge S, Gutierrez JA. SPARC: a potential diagnostic marker of invasive meningiomas. Clin Cancer Res 1999;5:237–41.

50. Lloyd RV, Johnson TL, Blaivas M, Sisson JC, Wiksibm BS. Detection of HLA-DR antigens in paraffin-embedded thyroid epithelial cells with a monoclonal antibody. Am J Pathol 1985;120:106–11.